phys. stat. sol. (a) **189**, No. 2, 269–275 (2002)

Structural and Magnetic Properties of Fe on $Cu_{84}Al_{16}(100)$

M. D. MARTINS[1]) and W. A. A. MACEDO

Laboratório de Física Aplicada, Centro de Desenvolvimento da Tecnologia Nuclear, CP 941, 30123-970 Belo Horizonte, MG, Brazil

(Received May 1, 2001; accepted September 30, 2001)

Subject classification: 61.14.Hg; 68.55.Jk; 75.70.Ak; S1.1

The structure and magnetism of epitaxial ultrathin Fe films deposited on $Cu_{84}Al_{16}(100)$ single crystal have been investigated by electron diffraction and surface magneto-optical Kerr effect (SMOKE). The correlation between structural and magnetic properties was explored for Fe films grown at two different temperatures, 160 K (LT) and 300 K (RT). The results show that the Fe films on $Cu_{84}Al_{16}(100)$ undergo a sensitive structural change, starting from a critical thickness, which depends on the deposition temperature. The critical thickness was estimated as ≈2 atomic monolayers (ML) and ≈10 ML for Fe films deposited at LT and RT, respectively. The SMOKE measurements show that the Fe films deposited at RT are non-magnetic up to ≈10 ML, whereas the Fe films deposited at LT are ferromagnetic, starting from ≈1.5 ML. The magnetic anisotropy of the LT-grown films changes from out-of-plane to in-plane at ≈3.5 ML Fe. The spin reorientation transition in the LT-grown Fe ultrathin films is connected to a fcc (100) to bcc (110) structural transformation.

Introduction The metastable fcc Fe stabilized as epitaxial ultrathin films at room temperature has been deeply explored for more than a decade and even today is a matter of significant interest in surface magnetism. Part of this interest is motivated by the complex magnetic behavior of fcc iron predicted by theoretical calculations for the dependence of the magnetic ground state and the magnetic moment (μ) versus atomic volume. As demonstrated by these calculations, fcc Fe (γ-Fe) should present strong magnetovolume instabilities; depending on the atomic volume the ground state of bulk metastable fcc Fe can be non-magnetic (NM), antiferromagnetic (AFM) or ferromagnetic (FM) with high and low magnetic moment [1, 2]. The lattice parameter determines the ground state of γ-Fe and a magnetovolume instability is predicted at 3.66 Å (or an atomic volume of 12.25 $Å^3$) indicating a first-order phase transition from the antiferromagnetic and low-spin ($1.1\mu_B$ per atom) phases to the ferromagnetic high-spin state ($\mu = 2.5\mu_B$ per atom). The magnetic moment of FM fcc Fe atoms increases monotonically with the lattice parameter [1–3]. Recent theoretical studies have predicted the existence of metastable spin states depending on the Fe thickness for ultrathin Fe films on different fcc substrates [4].

Experimentally, Fe on Cu(100) was the system chosen to stabilize fcc Fe as epitaxial ultrathin films at room temperature. Due to the small lattice misfit between Cu (3.615 Å at 20 °C) and fcc Fe (lattice parameter 3.59 Å at 20 °C, as extrapolated from the high temperature γ-Fe phase), the epitaxy of fcc Fe on Cu should be favored [5]. In fact, Fe/Cu(100) is a well-studied system which shows a complex correlation between magnetic and structural properties depending on the thickness of the Fe film and the growth conditions [5–11]. It was observed that magnetic and structural properties of Fe films deposited on Cu depend sensitively on deposition temperature [7] and prepara-

[1]) Corresponding author; Fax: +55 31 3499-3390; e-mail: mdm@cdtn.br

 0031-8965/02/18902-0269 $ 17.50+.50/0

tion procedure, as obtained by conventional thermal evaporation [6–10] or pulsed laser deposition [11]. Fcc Fe can be obtained by epitaxial growth on other suitable fcc substrates to vary the atomic volume of the fcc Fe phase regarding to Cu. Fe on Cu-Au alloys [12–15] and on Co [16], among others, represent an expansion of the lattice parameter in relation to Fe/Cu(100), and diamond (100) [17] represents a contraction of the Fe lattice. We studied ultrathin Fe films grown on $Cu_{84}Al_{16}(100)$ [18, 19], a fcc substrate with a lattice parameter of 3.65 Å, which is 1% larger than pure Cu. The $Cu_{84}Al_{16}(100)$ substrate has a lattice parameter between Cu (3.61 Å) and Cu_3Au (3.74 Å). We chose $Cu_{84}Al_{16}(100)$ in order to favor the stabilization of the FM, high-spin phase of fcc Fe since its lattice parameter matches the calculated atomic volume of the ferromagnetic high-spin γ-Fe [1].

In previous studies, the magnetic properties of Fe monolayers (ML) grown on $Cu_{84}Al_{16}(100)$ were determined by linear magnetic dichroism in core level photoemission (LMDAD) [18] and surface magneto-optical Kerr effect (SMOKE) [19]. The results have shown that Fe films (1 to 6 ML thick) grown at 160 K on $Cu_{84}Al_{16}(100)$ present in-plane ferromagnetism starting from ≈2.5 ML, and that annealing at room temperature destroys the in-plane ferromagnetic order of these Fe films in a non-reversible way. Here, we present a complementary study on the structure and magnetism of Fe monolayers epitaxially deposited on $Cu_{84}Al_{16}(100)$ and discuss the correlation between the structural and magnetic properties of this system. The growth and structure of the Fe films were investigated by low energy electron diffraction (LEED) and reflection high-energy electron diffraction (RHEED). The magnetic properties were determined by SMOKE measurements in the longitudinal geometry and at magnetic fields up to 1300 Oe. The Fe films were deposited at two different temperatures, 160 K (LT-growth) and 300 K (RT-growth), and the magnetic properties were investigated at temperatures as low as 150 K. The changes of the structural and magnetic properties of the LT-grown films after a rapid annealing at room temperature were also investigated.

Experimental Procedures The film preparation and the analysis were carried out in an ultrahigh vacuum (UHV) system equipped with standard techniques for deposition and analysis of thin films and surfaces including different evaporators, quartz microbalance, residual gas analyzer, X-ray photoelectron (XPS) and Auger electron spectroscopies (AES). In addition, electron diffraction techniques (LEED and RHEED) were used to study the film structure. The magnetic properties could be explored in situ by using a diode laser (670 nm) and an electromagnet mounted inside the vacuum chamber. The base pressure in the system was better than 2×10^{-10} mbar.

Epitaxial Fe overlayers (<13 ML thick) were grown under molecular beam epitaxy conditions onto a clean $Cu_{84}Al_{16}(001)$ substrate by electron beam evaporation of a high purity Fe wire (99.99%). The Fe films were grown at two different temperatures, 160 K (LT) and room temperature (RT), and the deposition rate was typically ≈0.5 ML/min. The surface of the substrate was previously prepared by cycles of Ar^+ sputtering at 1 keV and annealing at temperatures between 350 and 450 °C. This preparation procedure was repeated until a clean and well-ordered surface was obtained, as confirmed by AES and LEED, respectively. No contamination signal (C, O, S) was detected in the freshly prepared Fe films, as determined by AES. Reflection high-energy electron diffraction (electron energy up to 15 keV) was used to investigate the growth mode, thickness and structure of the ultrathin Fe films. A recording system with a CCD camera, a

S-VHS video recorder and a dedicated software for the data processing (eeScan-RL) completed the RHEED setup. In this way, the electron diffraction patterns of the surface were recorded while depositing Fe, and were further analyzed. The structure of the deposited films was also investigated by intensity measurements of the LEED specular beam versus electron energy (LEED $I_{00}(V)$ curves). Due to the SMOKE setup in a longitudinal configuration (s-polarized light reaching the film at 45° and signal detection near the extinction, i.e. crossed polarizers condition), the Kerr signal depends both on the longitudinal and polar magnetization components [20]. After growth and SMOKE measurements, films grown at LT were submitted to a rapid annealing up to room temperature (≈30 min of total heating time, 10 min at room temperature) and the structural and magnetic properties were then measured again at 160 K.

Results and Discussion Figure 1 presents typical evolutions of the in-plane lateral spacing a_L of the Fe films during deposition at 160 and 300 K, as determined by RHEED. The in-plane lateral spacing is inversely proportional to the distance between two adjacent diffraction streaks in the RHEED patterns. Each point plotted in this figure represents the relative variation of the in-plane lateral spacing in the Fe film as compared to the lateral spacing of the $Cu_{84}Al_{16}(100)$ surface (3.65 Å). The evolution of a_L during the Fe film growth was obtained from the electron diffraction patterns stored during the deposition. As can be seen in Fig. 1, for LT-growth the in-plane lateral spacing does not change up to about ≈2 ML of Fe and matches the substrate lattice parameter. Above this thickness, a progressive increase of this distance is observed and at ≈5.5 ML of Fe, a value 8% larger than that of the substrate is reached. For the room temperature deposition, the Fe film grows epitaxially on $Cu_{84}Al_{16}(100)$ with a small in-plane contraction (less than 1%). The in-plane lateral spacing starts to increase around a critical thickness of 10 ML of Fe, reaching ≈7% expansion at 13 ML. Moreover, it has been observed that the measured lateral expansion is connected to a significant change in the relative intensities of the RHEED $(\bar{1}, 0)$ and $(1, 0)$ streaks [21]. This change suggests a small rotation in the growth direction of the Fe film, as observed for Fe on Cu(100) [8].

The average vertical interplanar distance of the Fe atoms in the films was determined by LEED. The (00) diffraction beam intensity curves were collected as a function of the electron energy (LEED $I_{00}(V)$ curves) after film deposition and a kinematic approximation was used to calculate the vertical interplanar distance [22]. The periodic peak

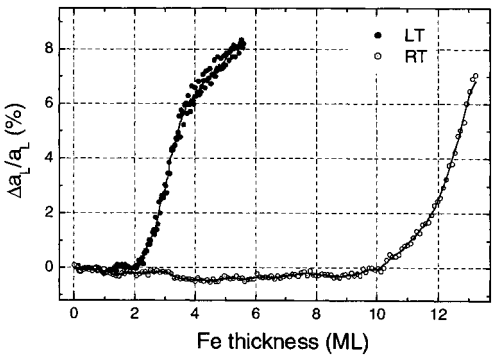

Fig. 1. Evolution of the in-plane lateral spacing a_L during deposition of Fe on $Cu_{84}Al_{16}(100)$ at 160 K (LT) and 300 K (RT), as determined by RHEED. $\Delta a_L/a_L$ represents the variation of a_L with respect to the clean substrate

sequence observed in LEED $I_{00}(V)$ curves corresponds to the constructive interference condition for the electron wave (Bragg condition). Considering that the electrons suffer only simple scattering in the diffraction process (the kinematic approximation), the electron energy E that satisfies the Bragg condition is linearly correlated to the square of the Bragg peak index n, as shown by the expression

$$E(n^2) = \frac{1}{8m}\left(\frac{h}{a_p \sin\theta}\right)^2 n^2 + V_0\,, \tag{1}$$

where V_0 is the additional energy shift due to the average inner potential in the crystal, m the electron mass, and θ the incident angle with respect to the sample surface. Therefore, the vertical interplanar spacing a_p can be evaluated by a linear fitting of the $E \times n^2$ points extracted from the $I_{00}(V)$ curves. The kinematical approach of the LEED $I(V)$ curves was recently investigated and validated in a study of the Co(10$\bar{1}$0) surface [23].

Figure 2a shows, as an example of the kinematic approach, LEED $I_{00}(V)$ curves for the clean surface of the $Cu_{84}Al_{16}(100)$ substrate, for 5.6 ML and 13 ML thick Fe films on $Cu_{84}Al_{16}(100)$, deposited at 160 and 300 K, respectively. The energetic positions of the Bragg peak sequences in each LEED curve versus n^2 are plotted in Fig. 2b. The straight lines represent linear regression fittings based on a kinematic approximation of the (00) diffraction beam intensity. Taking the slope of these linear fitting curves, the average vertical interplanar distance a_p was evaluated as described above. The experimental values obtained for the interplanar distance of the $Cu_{84}Al_{16}(100)$ substrate is 1.86 $\pm$ 0.03 Å. The results for the 5.6 ML (LT) and 13 ML (RT) thick Fe films grown on $Cu_{84}Al_{16}(100)$ are 2.01 $\pm$ 0.03 Å and 2.06 $\pm$ 0.03 Å, respectively.

The dependence of the vertical interplanar distance on the film thickness for LT- and RT-deposited Fe films on $Cu_{84}Al_{16}(100)$ is displayed in Fig. 3. For LT-deposited films, the LEED results show a linear increase of the interplanar distance, starting from 2 ML Fe, and a value 8% larger than the substrate interplanar distance is observed for a ≈5.5 ML thick Fe film. The interplanar distance shows a distinct behavior for the Fe films grown at RT. The values obtained for ≈6 and ≈8 ML thick Fe films show a small contraction relative to the substrate, while a 13 ML thick film is expanded by

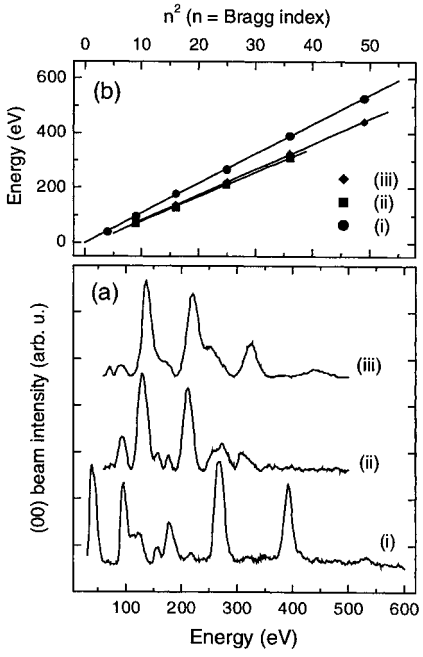

Fig. 2. a) LEED $I_{00}(V)$ curves for (i) the clean surface of the $Cu_{84}Al_{16}(100)$ substrate, and for a (ii) 5.6 ML and (iii) 13 ML thick Fe films on $Cu_{84}Al_{16}(100)$ deposited at 160 K and 300 K, respectively. b) $E(n^2)$ points relative to these $I(V)$ curves, where the straight lines represent linear regression fittings based on a kinematic approximation for the energy position of the diffraction Bragg peaks, as described in the text

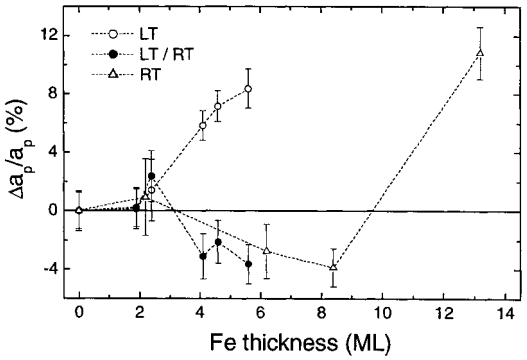

Fig. 3. Vertical interplanar distance a_p versus thickness of Fe films deposited on $Cu_{84}Al_{16}(100)$ at 160 K (LT, open circles) and 300 K (RT, open triangles). Values of a_p for the LT-grown films after the thermal treatment at room temperature are also presented (LT/RT, solid circles). The dashed lines are guides to the eye

11% with respect to the interplanar distance of the clean substrate. It must be observed that this structural evolution resembles the evolution of the lateral spacing with increasing Fe thickness, shown in Fig. 1, and it is evidence of a structural transformation within the Fe films during the film growth for both deposition temperatures. The RHEED and LEED results, i.e. the lattice expansion and the small rotation in the growth direction, suggest that for low temperature growth, starting from ≈2 ML, as the Fe thickness increases up to ≈5 ML, the structure of the Fe film changes from fcc-like [100] to a bcc-like [110], as also observed for the growth of Fe on Cu(100) at low temperature [8, 24]. For the films deposited at room temperature, an initial slightly contracted phase is observed up to ≈10 ML, when a similar structural transformation starts within the deposited Fe films.

Effects of rapid annealing at room temperature on the in-plane lateral and interplanar distances of Fe films deposited at 160 K were also investigated by RHEED and LEED measurements. Due to this annealing, the Fe films preserve the lateral spacing within ±2% and a clear contraction of the interplanar distance is observed, to a distance very close to that of the $Cu_{84}Al_{16}(100)$ substrate, as shown in Fig. 3.

The magnetic properties of the ultrathin Fe films were investigated in situ by longitudinal SMOKE at temperatures as low as 150 K. No longitudinal Kerr hysteresis loops were observed for the Fe films grown on $Cu_{84}Al_{16}(100)$ at room temperature. This result is in accordance with previously reported LMDAD data [18]. It was also observed by conversion electron Mössbauer spectroscopy (CEMS) that a 5 ML thick ^{57}Fe film deposited at RT on $Cu_{84}Al_{16}(100)$ presents a non-magnetic spectrum at 300 and 35 K [25]. Figure 4 shows typical longitudinal SMOKE loops for Fe films (<6 ML thick) on $Cu_{84}Al_{16}(100)$, measured at 150 K, immediately after deposition and in an applied magnetic field up to 300 Oe, as calibrated with a Hall probe. The results show that the LT-grown Fe films are ferromagnetic for thicknesses greater than ≈1.5 ML. The Kerr hysteresis loops are rounded and show a relatively large coercivity, which decreases with increasing Fe thickness up to 2.8 ML. Starting from ≈3.5 ML, clear square hysteresis loops can be observed. The SMOKE intensity increases linearly with Fe thickness while the coercivity remains constant around 100 Oe. The sharp reduction observed in the intensity of the loops between 2.8 and 3.5 ML Fe is indication of a spin reorientation transition. For thicknesses >3.5 ML, the ultrathin Fe films on $Cu_{84}Al_{16}(100)$ are present in-plane easy axis, in rough agreement with previous LMDAD results [18]. Moreover, by comparing Figs. 1 and 4, our results show that the onset of in-plane ferromagnetism in LT-grown films is clearly connected to the onset of expansion of the lateral spacing, i.e. of distortion of the fcc-like

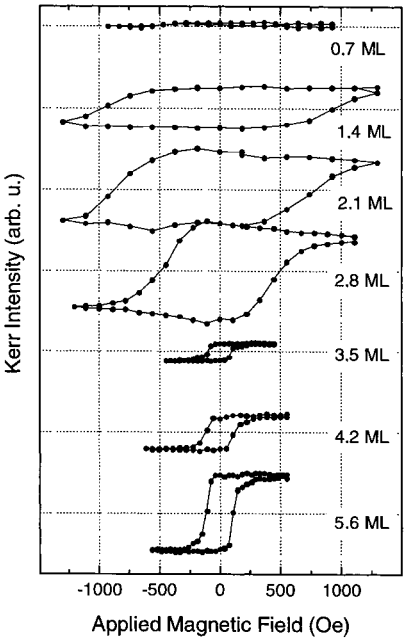

Fig. 4. Evolution with thickness of the longitudinal SMOKE hysteresis loops for ultrathin Fe films on $Cu_{84}Al_{16}(100)$, grown and measured at 140 K

structure. The observed magnetic behavior, i.e. the initial large coercivity which decreases abruptly to a constant value (≈100 Oe), suggests a spin reorientation from out-of-plane to in-plane magnetization within the Fe films at ≈3.5 ML. After annealing at RT, no magnetic loop has been obtained at LT, presumably due to the observed interplanar contraction and to Al interdiffusion [18].

Conclusion In conclusion, the growth, and the structural and magnetic properties of ultrathin Fe films deposited on $Cu_{84}Al_{16}(100)$ were investigated by RHEED, LEED, and longitudinal SMOKE. At low temperature (160 K), the epitaxial growth of Fe on $Cu_{84}Al_{16}(100)$ is pseudomorphic up to ≈2 ML and, as the Fe thickness increases from 2 to 5 ML, a gradual lattice expansion occurs. This is consistent with a structural transition from fcc-like (100) to bcc-like (110), similar to what is observed for Fe films grown on Cu(100) at low temperature. The onset of in-plane ferromagnetic order at ≈3.5 ML is connected to the observed structural transition. For annealing at room temperature, the lack of ferromagnetic order could be related not only to Al interdiffusion, as observed in reference [18], but also to the contraction of the interplanar spacing. For RT-deposition, the in-plane and interplanar distances are contracted relative to the $Cu_{84}Al_{16}(100)$ substrate up to 10 ML of Fe. The MOKE results show that the RT-grown Fe films are non-magnetic (or antiferromagnetic with $T_N < 35$ K) up to 10 ML of Fe. These results suggest the growth of γ-Fe overlayers on $Cu_{84}Al_{16}(100)$ at room temperature up to a critical thickness of ≈10 ML. Above the critical thickness, a structural transformation (fcc → bcc) occurs.

Acknowledgements The authors gratefully acknowledge the financial support of the Brazilian Agencies CNEN, CNPq and Fapemig.

References

[1] V. L. MORUZZI, P. M. MARCUS, and J. KÜBLER, Phys. Rev. B **39**, 6957 (1989), and references therein.
[2] T. KRAFT, P. M. MARCUS, and M. SCHEFFLER, Phys. Rev. B **49**, 11511 (1994).
[3] D. GUENZBURGER and D. E. ELLIS, Phys. Rev. B **51**, 12519 (1995).
[4] T. ASADA and S. BLÜGEL, Phys. Rev. Lett. **79**, 507 (1997).
R. LORENZ and J. HAFNER, Phys. Rev. B **58**, 5197 (1998).
E. G. MORONI, G. KRESSE, and J. HAFNER, J. Phys.: Condens. Matter **11**, L35 (1999).
P. M. MARCUS, V. L. MORUZZI, and S.-L. QIU, Phys. Rev. B **60**, 369 (1999).

M. Friak, M. Šob, and V. Vitek, Phys. Rev. B **63**, 052405 (2001).
[5] S. H. Lu, J. Quinn, D. Tian, F. Jona, and P. M. Marcus, Surf. Sci. **209**, 364 (1989).
[6] W. A. A. Macedo and W. Keune, Phys. Rev. Lett. **61**, 475 (1988).
[7] D. Li, M. Freitag, J. Pearson, Z. Q. Qiu, and S. D. Bader, Phys. Rev. Lett. **72**, 3112 (1994).
[8] S. Müller, P. Bayer, C. Reischl, K. Heinz, B. Feldmann, H. Zillgen, and M. Wuttig, Phys. Rev. Lett. **74**, 765 (1995).
[9] R. D. Ellerbrock, A. Fuest, A. Schatz, W. Keune, and R. A. Brand, Phys. Rev. Lett. **74**, 3053 (1995).
[10] M. Zharnikov, A. Dittschar, W. Kuch, C. M. Schneider, and J. Kirschner, Phys. Rev. Lett. **76**, 4620 (1996).
[11] H. Jenniches, J. Shen, Ch. V. Mohan, S. Sundar Manoharan, J. Barthel, P. Ohresser, M. Klaua, and J. Kirschner, Phys. Rev. B **59**, 1196 (1999).
[12] R. Rochow, C. Carbone, Th. Dodt, F. P. Johnen, and E. Kisker, Phys. Rev. B **41**, 3426 (1990).
[13] W. A. A. Macedo, W. Keune, and R. D. Ellerbrock, J. Magn. Magn. Mater. **93**, 552 (1991).
[14] D. J. Keavney, D. F. Storm, J. W. Freeland, I. L. Grigorov, and J. C. Walker, Phys. Rev. Lett. **74**, 4531 (1995).
[15] F. Baudelet, M.-T. Lin, W. Kuch, K. Meinel, B. Choi, C. M. Schneider, and J. Kirschner, Phys. Rev. B **51**, 12563 (1995).
M.-T. Lin, J. Shen, W. Kuch, H. Jenniches, M. Klaua, C. M. Schneider, and J. Kirschner, Phys. Rev. B **55**, 5886 (1997).
[16] W. L. O'Brien and B. P. Tonner, Surf. Sci. **334**, 10 (1995).
[17] D. Li, D. J. Keavney, J. Pearson, S. D. Bader, J. Pege, and W. Keune, Phys. Rev. B **57**, 10004 (1998).
[18] W. A. A. Macedo, F. Sirotti, A. Schatz, D. Guarisco, G. Panaccione, W. Keune, and G. Rossi, J. Magn. Magn. Mater. **177–181**, 1262 (1998).
W. A. A. Macedo, F. Sirotti, G. Panaccione, A. Schatz, W. Keune, W. N. Rodrigues, and G. Rossi, Phys. Rev. B **58**, 11534 (1998).
[19] M. D. Martins, L. H. F. Andrade, P. L. Gastelois, and W. A. A. Macedo, J. Appl. Phys. **89**, 6680 (2001)
[20] Z. Q. Qiu and S. D. Bader, J. Magn. Magn. Mater. **200**, 664 (1999), and references therein.
[21] M. D. Martins, Ph. D. Thesis, Federal University of Minas Gerais, Belo Horizonte (Brazil) 2001.
[22] J. B. Pendry, Low Energy Electron Diffraction, Academic Press, New York 1974.
[23] A. Barbier, P. Ohresser, V. da Costa, B. Carriere, and J.-P. Deville, Surf. Sci. **405**, 298 (1998).
[24] H. Zillgen, B. Feldmann, and M. Wuttig, Surf. Sci. **321**, 32 (1994).
[25] A. Schatz, Ph.D. Thesis, Duisburg University, Duisburg (Germany) 1996.